Electronic Supplementary Information (ESI)

Regulation of aggregation-induced emission behaviours and mechanofluorochromism of tetraphenylethene through different oxidation states of sulphur moieties

*Qin Yang,[a] Dongyang Li, [b] Weijie Chi,[c] Ronghui Guo,[a] Bin Yan,[a] Jianwu Lan,[*a] Xiaogang Liu[*c] and Jun Yin[*b,d]*

[a]College of Light Industry and Textile and Food Engineering, Sichuan University, Chengdu, Sichuan, 610005, China

[b]Key Laboratory of Pesticide and Chemical Biology, Ministry of Education, College of Chemistry, Central China Normal University, Wuhan 430079, P. R. China.

[c]Singapore University of Technology and Design, 8 Somapah Road, Singapore 487372. E-mail: xiaogang_liu@sutd.edu.sg

[d]State Key Laboratory of Chemical Oncogenomics, Key Laboratory of Chemical Biology, the Graduate School at Shenzhen, Tsinghua University, Shenzhen, Guangdong, PR China, 518055

Contents:

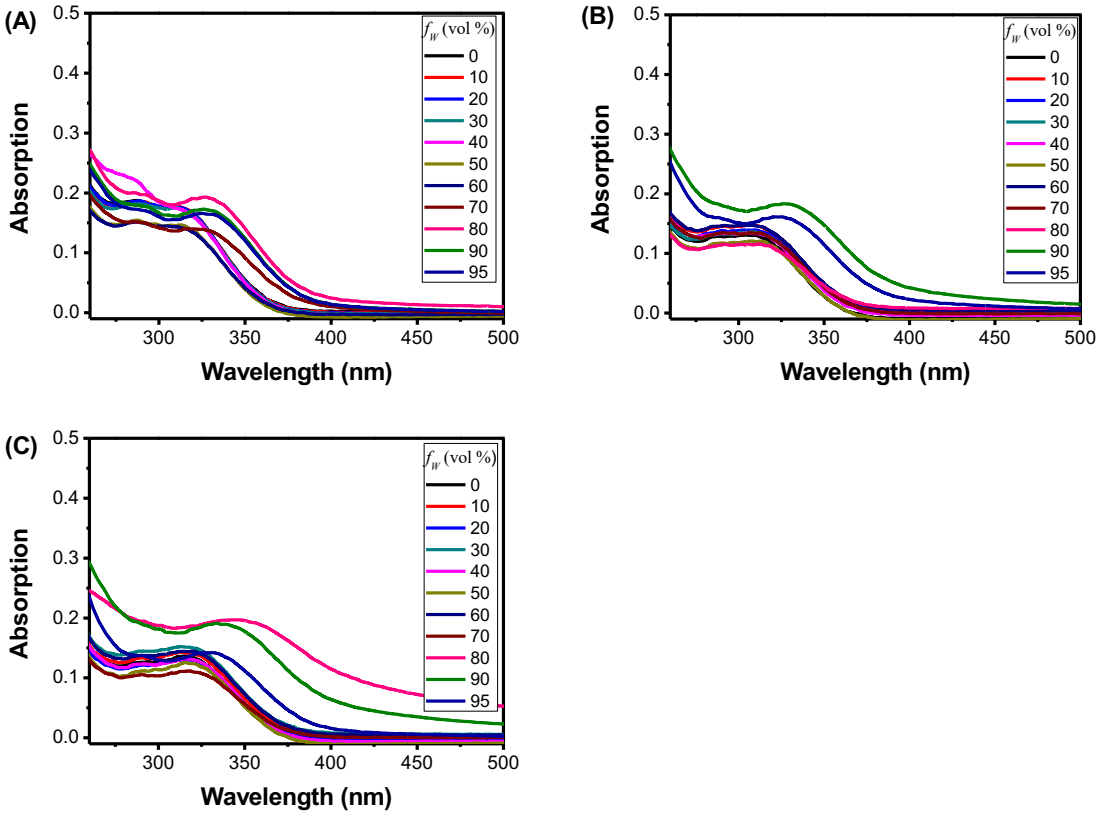

Fig. S1. The UV-Vis absorption spectra **1** (A), **2** (B), and **3** (C) (10 μM) in CH_3CN-H_2O mixtures with different volume fractions of water (f_W).

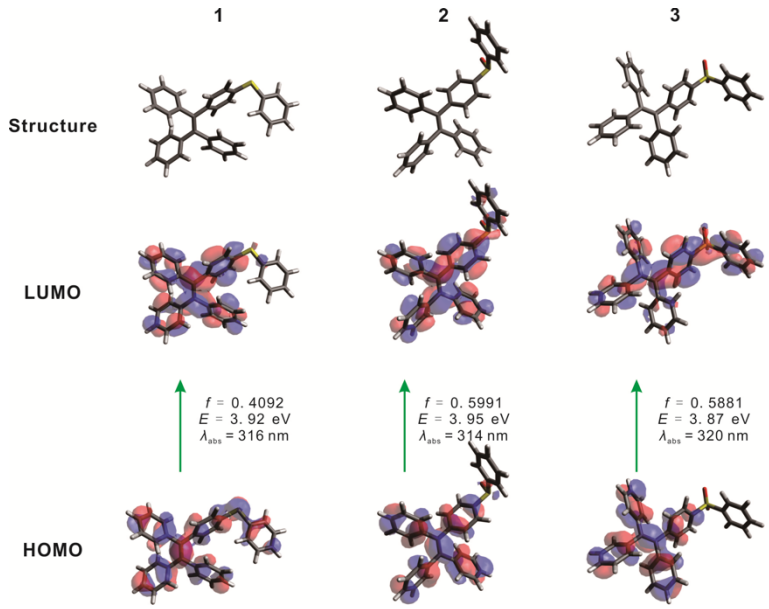

Fig. S2. Optimized molecular structures and frontier molecular orbitals, as well as their photoexcitation data (*f*: oscillator strength; *E*: excitatio energy from the S_0 to the S_1 state; λ_{abs}: calculated peak UV-vis absorption wavlengths) of **1**—**3** in water.

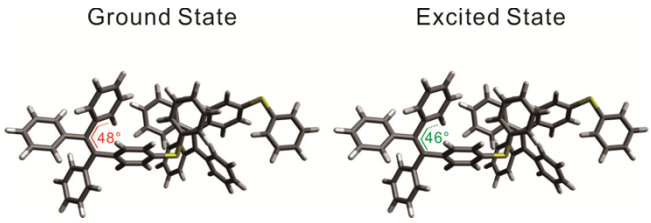

Fig. S3. Optimized dimer structures of **1** and one selected dihedral angel of a phenyl ring both in the ground (S_0) and the first excited singlet states (S_1) in water.

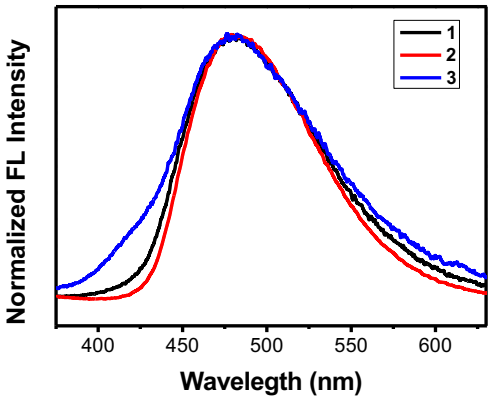

Fig. S4. The Normalized fluorescence emission spectra (λ_{ex} = 340 nm) of **1**, **2** and **3** in the amorphous phase.

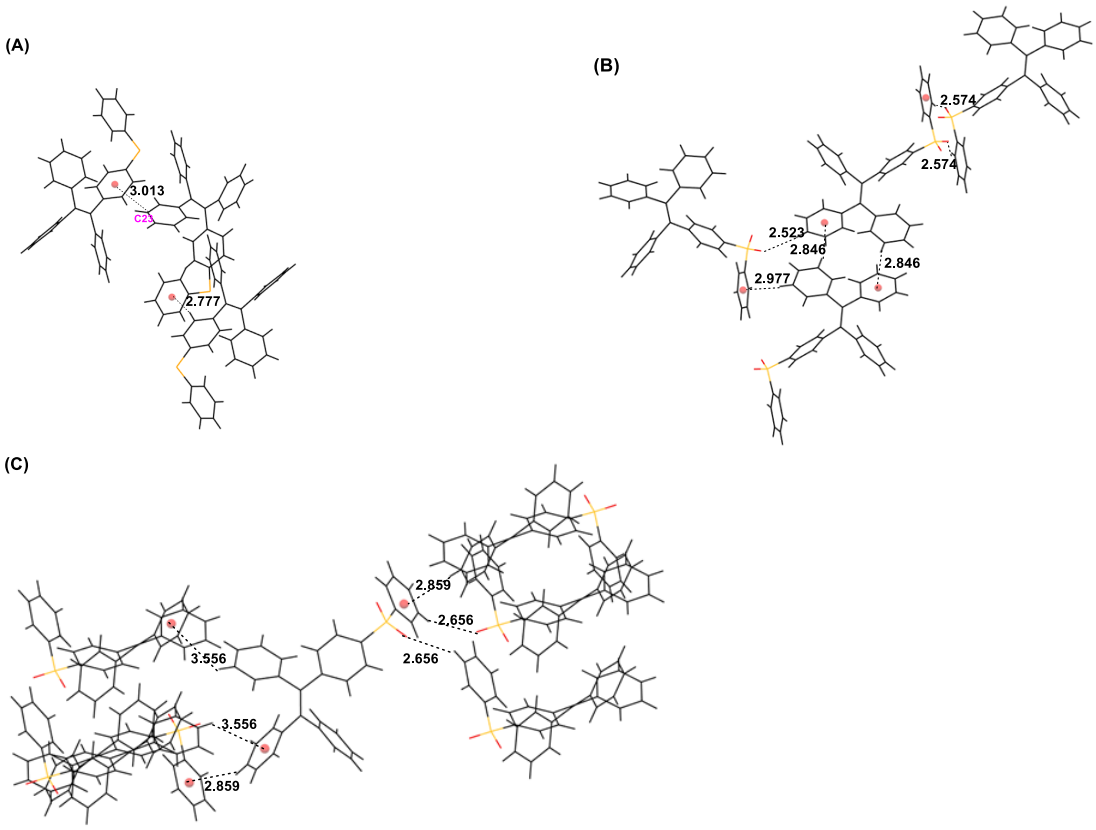

Fig. S5. The intermolecular interactions in the crystals of **1** (A), **3W** (B), and **3G** (C).

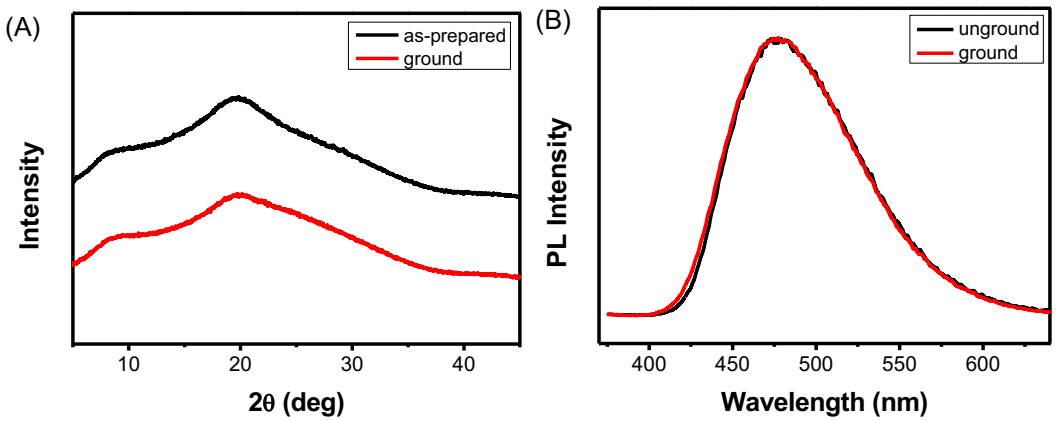

Fig. S6. The XRD patterns (A) and PL spectra (B) of **2.** Excitation wavelength: 340 nm.

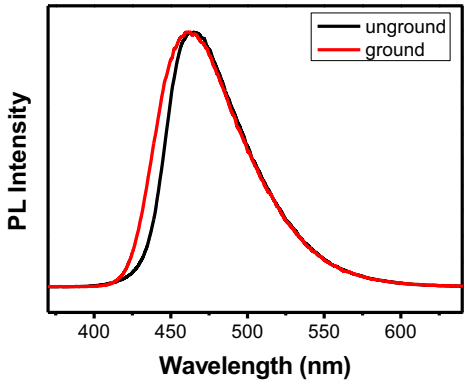

Fig. S7. The PL spectra of **3G** before and after grinding. Excitation wavelength: 340 nm.

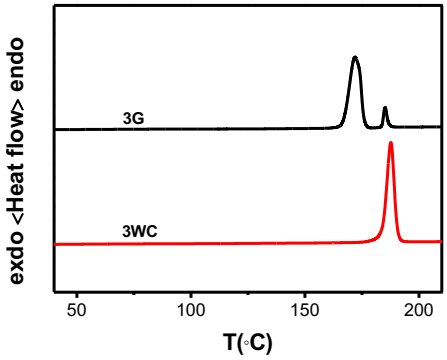

Fig. S8. DSC curves of **3G** and **3W**.

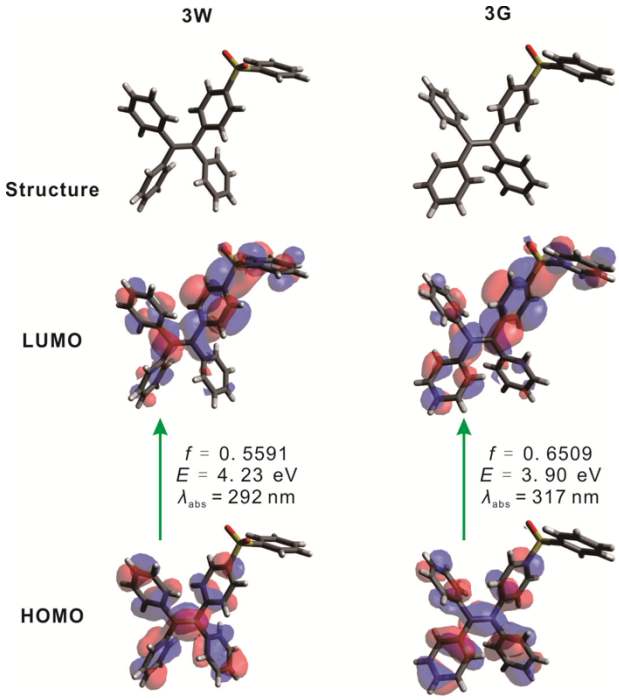

Fig. S9. Molecular structures of **3W** and **3G** as extracted from crystal structures, their frontier molecular orbitals, and photoexcitation data in water (*f*: oscillator strength; *E*: excitatio energy from the S_0 to the S_1 state; λ_{abs}: calculated peak UV-vis absorption wavlengths).

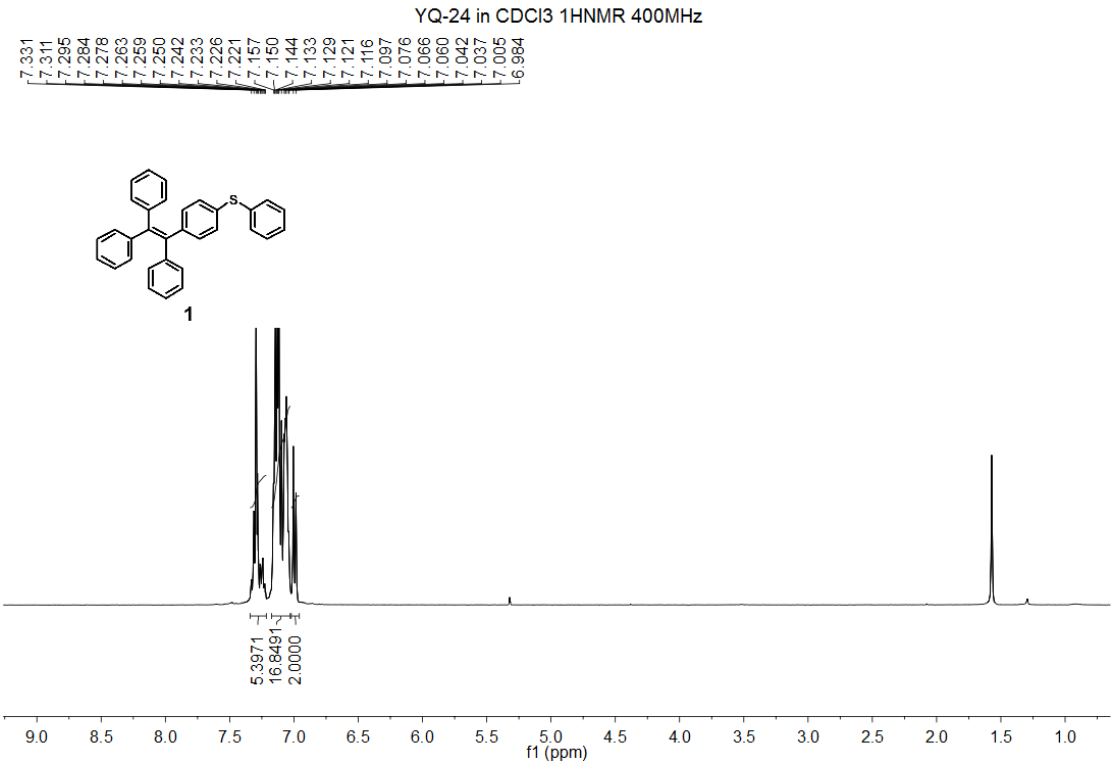

Fig S10. ^{1}H NMR of **1** in $CDCl_3$.

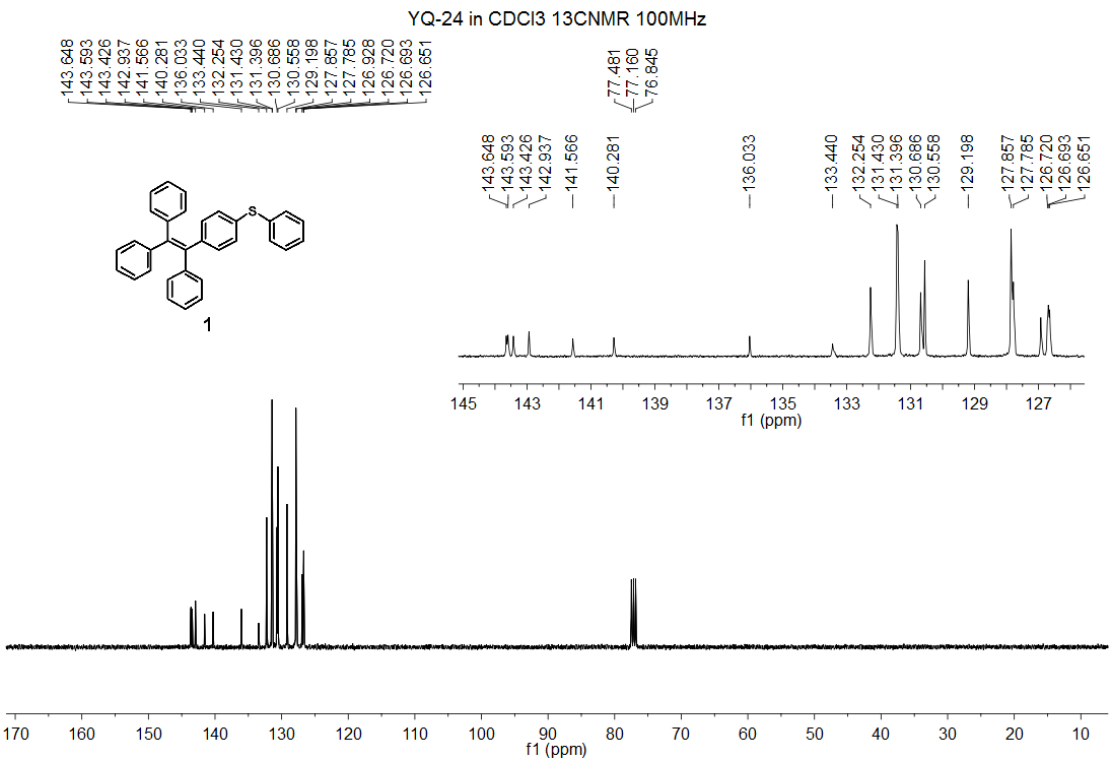

Fig S11. ^{13}C NMR of **1** in $CDCl_3$.

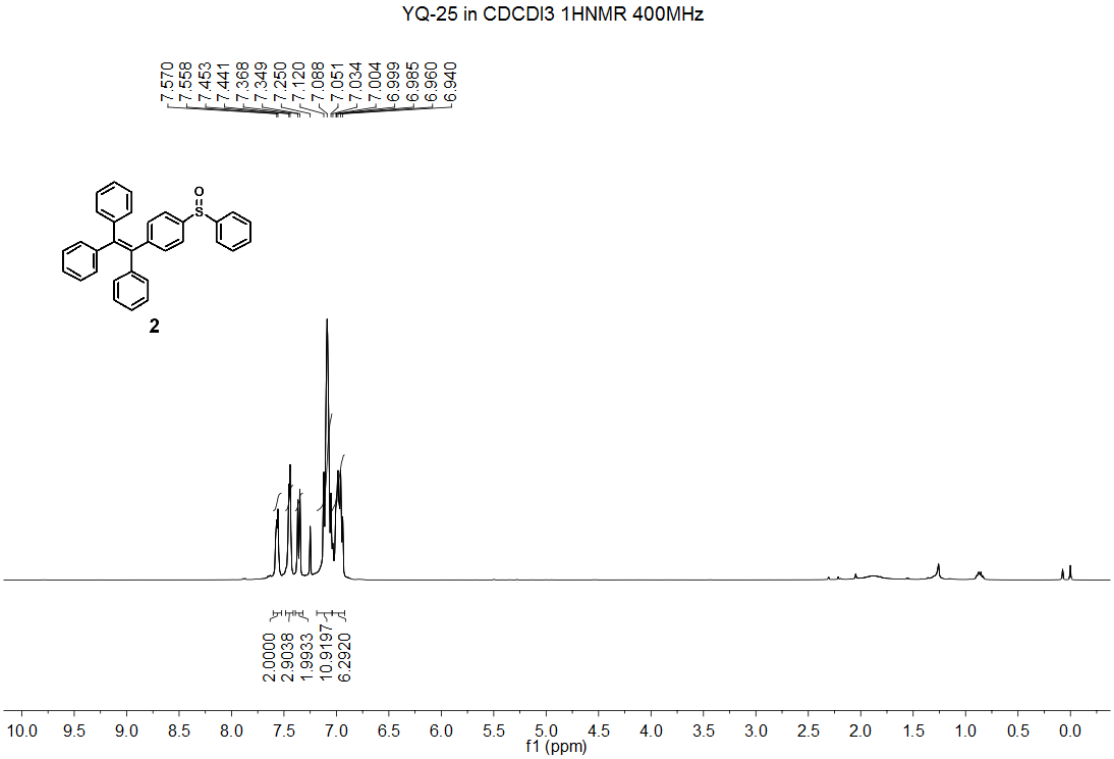

Fig S12. ^{1}H NMR of **2** in $CDCl_3$.

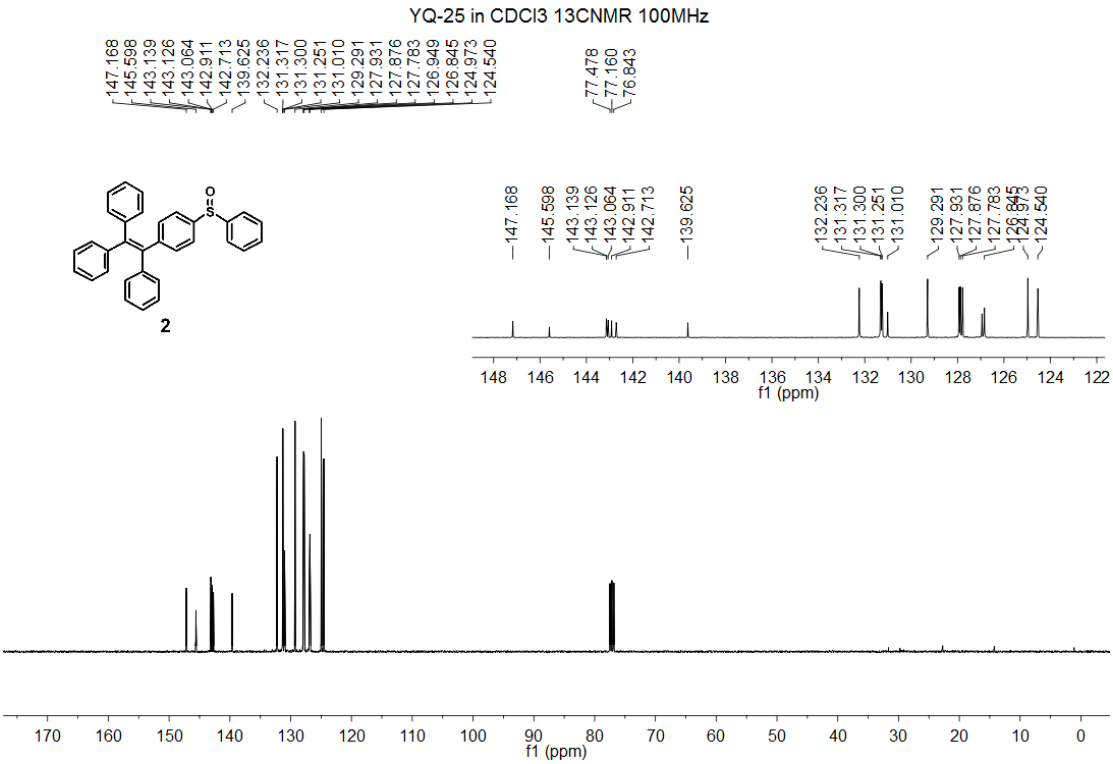

Fig S13. ^{13}C NMR of **2** in $CDCl_3$.

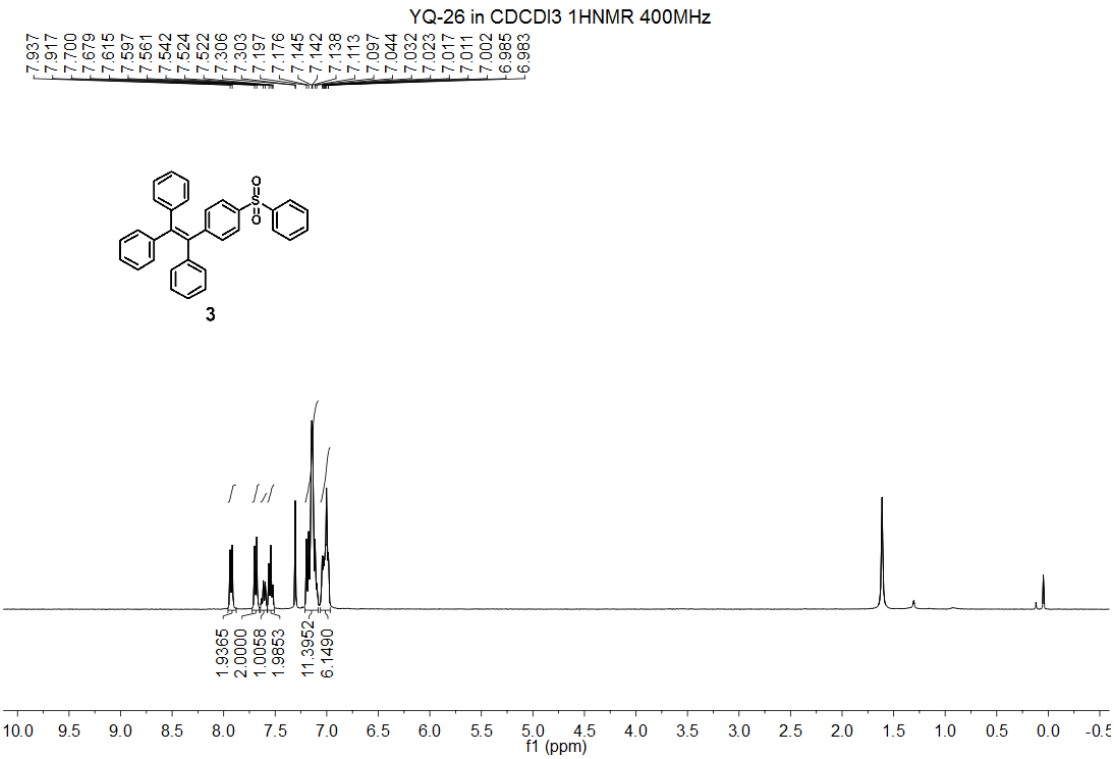

Fig S14. ^{1}H NMR of **3** in $CDCl_3$.

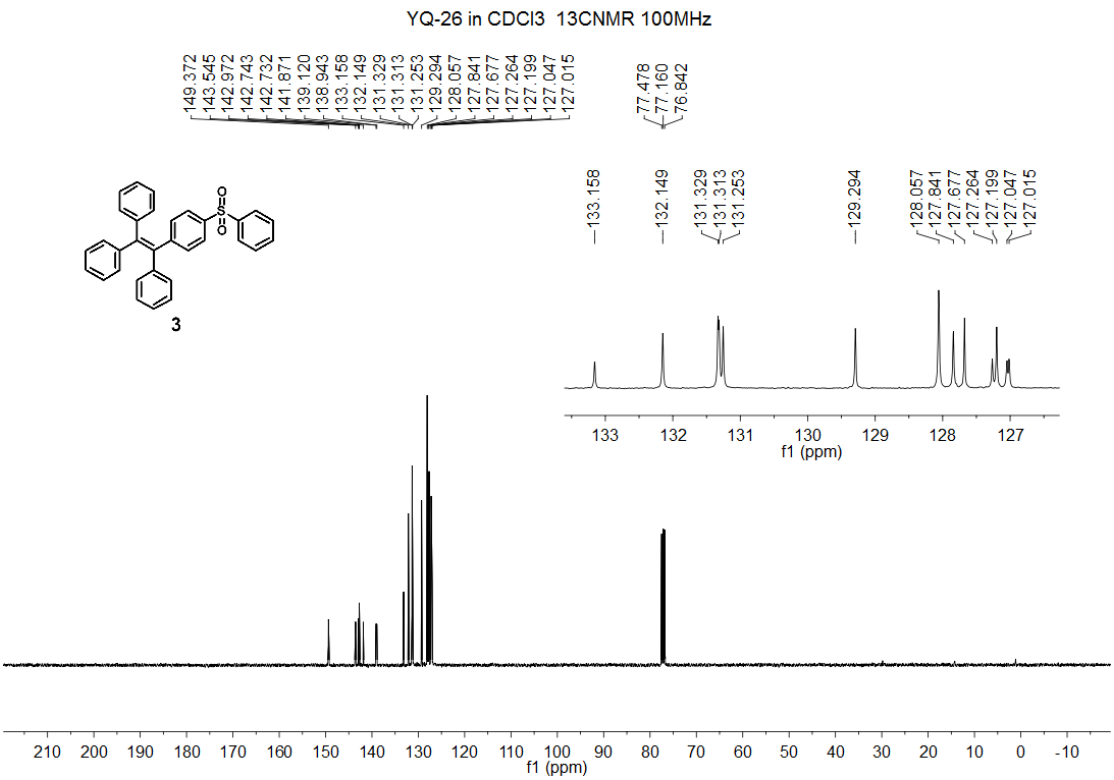

Fig S15. ^{13}C NMR of **3** in $CDCl_3$.

Table S1. Crystal data and structure refinement for **1**.

Identification code	**1**
Empirical formula	$C_{32}H_{24}S$
Formula weight	440.57
Temperature/K	293.15
Crystal system	orthorhombic
Space group	Pbca
a/Å	14.9419(11)
b/Å	17.6599(17)
c/Å	18.1494(18)
α/°	90
β/°	90
γ/°	90
Volume/Å^3	4789.1(7)
Z	8
ρ_{calc}g/cm^3	1.222
μ/mm^{-1}	0.153
F(000)	1856.0
Crystal size/mm^3	0.3 × 0.3 × 0.25
Radiation	MoKα (λ = 0.71073)
2Θ range for data collection/°	6.332 to 52.738
Index ranges	-18 ≤ h ≤ 18, -13 ≤ k ≤ 22, -22 ≤ l ≤ 20

Reflections collected	13409
Independent reflections	4881 [R_{int} = 0.0618, R_{sigma} = 0.0909]
Data/restraints/parameters	4881/0/298
Goodness-of-fit on F^2	0.955
Final R indexes [I>=2σ (I)]	R_1 = 0.0776, wR_2 = 0.1897
Final R indexes [all data]	R_1 = 0.1545, wR_2 = 0.2356
Largest diff. peak/hole / e $Å^{-3}$	0.31/-0.31

Table S2. Crystal data and structure refinement for **3G** and **3W.**

Identification code	**3G**	**3W**
Empirical formula	$C_{32}H_{24}O_2S$	$C_{32}H_{24}O_2S$
Formula weight	472.57	472.57
Temperature/K	293.15	293.15
Crystal system	monoclinic	monoclinic
Space group	$P2_1/n$	$P2_1/c$
a/Å	12.8357(4)	13.7068(13)
b/Å	8.1876(3)	16.8217(15)
c/Å	24.0614(9)	11.5705(11)
α/°	90	90
β/°	94.159(3)	105.319(10)
γ/°	90	90
Volume/$Å^3$	2522.03(16)	2573.0(4)
Z	4	4
ρ_{calc}g/cm^3	1.245	1.220
μ/mm^{-1}	0.155	0.152
F(000)	992.0	992.0
Crystal size/mm^3	0.35 × 0.3 × 0.25	0.3 × 0.2 × 0.2
Radiation	MoKα (λ = 0.71073)	MoKα (λ = 0.71073)
2Θ range for data collection/°	5.906 to 52.744	5.886 to 52.744
Index ranges	-15 ≤ h ≤ 16, -10 ≤ k ≤ 9, -30 ≤ l ≤ 26	-15 ≤ h ≤ 17, -20 ≤ k ≤ 20, -14 ≤ l ≤ 14
Reflections collected	13857	7293
Independent reflections	5141 [R_{int} = 0.0233, R_{sigma} = 0.0338]	7293 [R_{int} = ?, R_{sigma} = 0.0550]
Data/restraints/parameters	5141/0/316	7293/0/317
Goodness-of-fit on F^2	1.022	0.915
Final R indexes [I>=2σ (I)]	R_1 = 0.0465, wR_2 = 0.1033	R_1 = 0.0432, wR_2 = 0.0891
Final R indexes [all data]	R_1 = 0.0685, wR_2 = 0.1140	R_1 = 0.0780, wR_2 = 0.0972
Largest diff. peak/hole / e $Å^{-3}$	0.25/-0.30	0.21/-0.28

Table S3. The selected torsion angles (°) among benzene rings and the plane of the ethylene within crystals of **3G** and **3W**.

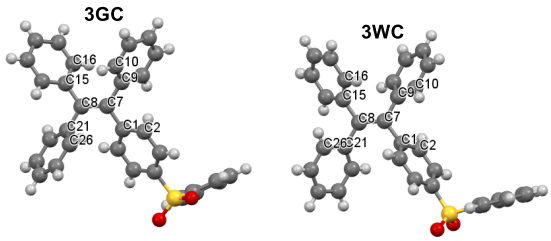

Crystal	**C7C8C15C16**	**C7C8C21C26**	**C8C7C9C10**	**C2C1C7C9**	**average**
3G	38.3	56.9	53.4	36.4	46.2
3W	-59.2	138.3	124.0	-54.7	52.9